

A 3D Stokes Framework for Wireless Depolarized Channels

Marcia Golmohamadi* and Jeff Frolik

Abstract—In severe multipath channels, depolarization of wireless signals has been shown to be a three dimensional effect. This work herein presents and applies a 3D Stokes vector framework for such depolarization. Empirical data are used to illustrate the capabilities of this framework (specifically, polarization purity indices and direction of propagation) to describe depolarization behavior for three different wireless channels.

1. INTRODUCTION

Wireless communication is becoming evermore pervasive with the advent of machine-to-machine (M2M) and other Internet of Things (IoT) systems. This pervasiveness leads to systems being deployed in environments that are less than ideal for wireless communications (e.g., about and/or within industrial machinery). Such environments can consist of a variety of surfaces that block and/or reflect the wireless signals thus introducing non-line-of-sight (NLOS) and/or multipath conditions, respectively. These conditions can cause not only fading in a channel but also depolarize the transmitted signal [1]. For point-to-point wireless communication systems with a strong line of sight (LOS), it is reasonable to state that there are only two relevant polarizations (e.g., vertical/horizontal linear or left/right hand circular polarization) which lie in the 2D plane normal to the direction of propagation. However, cluttered environments can lead to depolarization in a third dimension [2]. Thus, we contend and show herein, one should consider a 3D polarization framework versus a 2D one.

Electromagnetic wave polarization characterization in two dimensions is well studied. However, the description of electromagnetic waves in three dimensions, where in general there is no specific propagation direction, is still an open question which needs careful consideration [3, 4]. A well-defined polarization model will build a basis for understanding the input-to-output polarization behavior in wireless channels. Cross-polarization discrimination (XPD) has been used for polarization characterization [5], but this metric is not capable of fully interpreting polarization properties of electromagnetic waves. Thus, in this work we consider a Stokes vector framework. A 2D Stokes vector framework has been used to model polarization behavior in multipath channels before [6], but employing a 3D framework has received little attention. The 3D framework was been applied for analyzing propagation within reverberation chambers [7]. Herein, we extend this initial contribution by characterizing frequency-dependant polarization effects and the propagation direction in 3D and apply this framework to empirical data.

In this paper, we present, in Section 2, analytical frameworks by which 2D and 3D depolarization are described using a spectral polarization matrix. Further, we present and analyze empirical data, in Section 3, for three different environments finding their polarization indices and also their variations of propagation direction. The contributions of this work are summarized in Section 4.

Received 21 January 2019, Accepted 19 March 2019, Scheduled 30 March 2019

* Corresponding author: Marcia Golmohamadi (marcia.golmohamadi@uvm.edu).
The authors are with the University of Vermont, USA.

2. POLARIZATION FRAMEWORK

In this section, we review the 2D polarization framework and then extend it to the third dimension. At a fixed point in space, the electric field of an electromagnetic wave outlines a polarization ellipse perpendicular to the propagation direction. In an ideal environment (i.e., anechoic chamber), the polarization ellipse remains in a fixed plane and maintains its shape, whereas in a multipath environment not only the shape of polarization ellipse changes but also its plane and consequently direction of propagation vary over time/frequency/space. In the latter case, as our data will show, a 2D representation is no longer sufficient.

2.1. 2D Framework

A 2D coherency matrix, or polarization matrix, contains all information about autocorrelation and cross-correlation of the electric field components that are assumed to be contained in the x, y plane.

In this work, we consider the matrix elements in the space-frequency domain and call it the *spectral polarization matrix* which can be written as [8]

$$\Phi_{2D} = \begin{bmatrix} \langle E_x(r, f)E_x(r, f)^* \rangle & \langle E_x(r, f)\langle E_y(r, f)^* \rangle \rangle \\ \langle E_y(r, f)E_x^*(r, f) \rangle & \langle E_y(r, f)E_y(r, f)^* \rangle \end{bmatrix} \quad (1)$$

where, E_x and E_y are orthogonal components of the electric field vector at frequency f and position r and the asterisk denotes complex conjugation. The operator $\langle \rangle$ indicates that averaging of the signal has to be performed over the ensemble that characterizes the statistical properties of the field. Henceforth, we omit the explicit dependence on r and f . The spectral polarization matrix is non-negative definite Hermitian and consequently it is diagonalizable.

Any 2×2 diagonal representation of the spectral polarization matrix can be written as the sum of fully polarized $\rho_p = \text{diag}\{1, 0\}$ and completely unpolarized $\rho_{2u} = \frac{1}{2}\text{diag}\{1, 1\}$ matrices [9], that is

$$\Phi_{2D} = (\lambda_1 - \lambda_2)\rho_p + 2\lambda_2\rho_{2u} \quad (2)$$

where, λ_1 and λ_2 are eigenvalues of the matrix Φ_{2D} . The degree of polarization in a 2D framework, P , is a metric to measure depolarization extent in an environment and is defined as the ratio of the intensity of the fully polarized part of the field to the total intensity of the field [3]. P can also be obtained from Stokes parameters that will be described shortly.

$$P = \frac{\text{Tr}((\lambda_1 - \lambda_2)\rho_p)}{\text{Tr}(\Phi_{2D})} = \frac{\lambda_1 - \lambda_2}{\lambda_1 + \lambda_2} = \frac{\sqrt{\sum_{i=1}^3 \langle s_i \rangle^2}}{\langle s_0 \rangle} \quad (3)$$

where, Tr denotes the trace operation. Furthermore, the 2×2 identity matrix (σ_0) and the three Pauli spin matrices ($\sigma_1, \sigma_2, \sigma_3$) form a basis in which the spectral polarization matrix can be expanded as follows [10].

$$\Phi_{2D} = \frac{1}{2} \sum_{j=0}^3 \langle s_j \rangle \sigma_j \quad (4)$$

In this expansion, the coefficients, s_j , are the Stokes parameters. These parameters provide a convenient framework of representing polarization state of a wave and form a complete set that characterize any fixed-plane electromagnetic wave. The 2D Stokes vector, \mathbf{S}_{2D} , is defined as follows [11],

$$\mathbf{S}_{2D} = \begin{bmatrix} s_0 \\ s_1 \\ s_2 \\ s_3 \end{bmatrix} = \begin{bmatrix} |E_x|^2 + |E_y|^2 \\ |E_x|^2 - |E_y|^2 \\ E_x E_y^* + E_y E_x^* \\ -i(E_x E_y^* - E_y E_x^*) \end{bmatrix}. \quad (5)$$

The first parameter of Stokes vector, s_0 , is the intensity of the electromagnetic wave. The other three parameters, s_1 , s_2 , and s_3 describe the polarization state of the wave.

2D Stokes parameters can be geometrically represented in Poincare sphere. For example, pure linear polarizations lie on the equator of the sphere, where vertical and horizontal polarizations

are on diametrically opposite sides of the sphere. Any inner point of the sphere corresponds to a partially polarized wave. The origin represents a completely unpolarized wave that has the following characteristics: $\mathbf{S}_{2D} = [I, 0, 0, 0]^T$ (where I is the intensity of the field) and $P = 0$ (i.e., $\lambda_1 = \lambda_2$).

2.2. 3D Framework

In the presence of severe multipath, the polarization state of electromagnetic waves cannot be fully realized within a 2D framework (as we demonstrate in Section 3). Therefore, we now present the 3D spectral polarization matrix to describe wireless depolarization more generally [12].

$$\Phi_{3D} = \begin{bmatrix} \langle E_x E_x^* \rangle & \langle E_x E_y^* \rangle & \langle E_x E_z^* \rangle \\ \langle E_y E_x^* \rangle & \langle E_y E_y^* \rangle & \langle E_y E_z^* \rangle \\ \langle E_z E_x^* \rangle & \langle E_z E_y^* \rangle & \langle E_z E_z^* \rangle \end{bmatrix} \quad (6)$$

where the electric field vector has three orthogonal components along x, y, z axes. Unlike the 2D framework, Φ_{3D} cannot be described as the sum of only two components of a fully polarized and a fully unpolarized wave, as we had in Eq. (2). However, prior work [3] has shown that the diagonal representation of Φ_{3D} can be decomposed into three parts instead. Namely, fully polarized component $\rho_p = \text{diag}\{1, 0, 0\}$, fully 2D unpolarized $\rho_{2u} = \frac{1}{2} \text{diag}\{1, 1, 0\}$ and fully 3D unpolarized components $\rho_{3u} = \frac{1}{3} \text{diag}\{1, 1, 1\}$.

The decomposition of 3D spectral polarization matrix can be presented as

$$\Phi_{3D} = (\lambda_1 - \lambda_2)\rho_p + 2(\lambda_2 - \lambda_3)\rho_{2u} + 3\lambda_3\rho_{3u} \quad (7)$$

where, λ_1, λ_2 and λ_3 are eigenvalues of the 3D spectral polarization matrix, Φ_{3D} . Subsequent work [13] proposed two polarization indices, P_1 and P_2 , such that P_1 defines stability of polarization ellipse and P_2 represents stability of propagation direction or stability of polarization plane. P_1 is the ratio of the intensity of the fully polarized part of the field to the total intensity and P_2 is the ratio of components that have a fixed propagation direction (fully polarized and 2D unpolarized parts) to the total density of the field

$$P_1 = \frac{\text{Tr}((\lambda_1 - \lambda_2)\rho_p)}{\text{Tr}(\Phi_{3D})} = \frac{\lambda_1 - \lambda_2}{\lambda_1 + \lambda_2 + \lambda_3} \quad (8)$$

$$P_2 = \frac{\text{Tr}((\lambda_1 - \lambda_2)\rho_p + 2(\lambda_2 - \lambda_3)\rho_{2u})}{\text{Tr}(\Phi_{3D})} = \frac{\lambda_1 + \lambda_2 - 2\lambda_3}{\lambda_1 + \lambda_2 + \lambda_3} \quad (9)$$

In the 3D framework, the 3×3 identity matrix (ω_0) and eight Gell-Mann matrices ($\omega_1 \dots \omega_8$) form a basis for the 3D spectral polarization matrix such that [11]

$$\Phi_{3D} = \frac{1}{3} \sum_{j=0}^8 \langle \Lambda_j \rangle \omega_j \quad (10)$$

where, the nine real coefficients Λ_j are the generalized Stokes parameters of the 3D Stokes vector (\mathbf{S}_{3D}) [11]

$$\mathbf{S}_{3D} = \begin{bmatrix} \Lambda_0 \\ \Lambda_1 \\ \Lambda_2 \\ \Lambda_3 \\ \Lambda_4 \\ \Lambda_5 \\ \Lambda_6 \\ \Lambda_7 \\ \Lambda_8 \end{bmatrix} = \begin{bmatrix} |E_x|^2 + |E_y|^2 + |E_z|^2 \\ 3/2(E_x E_y^* + E_y E_x^*) \\ i3/2(E_x E_y^* - E_y E_x^*) \\ 3/2(|E_x|^2 - |E_y|^2) \\ 3/2(E_x E_z^* + E_z E_x^*) \\ i3/2(E_x E_z^* - E_z E_x^*) \\ 3/2(E_y E_z^* + E_z E_y^*) \\ i3/2(E_y E_z^* - E_z E_y^*) \\ \sqrt{3/4}(|E_x|^2 + |E_y|^2 - 2|E_z|^2) \end{bmatrix} \quad (11)$$

Some analogies can be made between 2D and 3D Stokes parameters. Λ_0 , which is the intensity of the wave, is analogous to s_0 in the 2D framework. Λ_1, Λ_2 , and Λ_3 in the 3D formulation are analogous to s_2, s_3 , and s_1 , respectively, in 2D. Furthermore, the pair of (Λ_4, Λ_5) and (Λ_6, Λ_7) can be compared to

(s_2, s_3) in different plane coordinates. Furthermore, it has been shown that the direction of propagation (\mathbf{V}) can be defined from 3D Stokes parameters as follows [8]

$$\mathbf{V} = (-\Lambda_7, \Lambda_5, \Lambda_2), \quad \phi = \arctan \frac{\Lambda_5}{-\Lambda_7}, \quad \theta = \arccos \frac{\Lambda_2}{|\mathbf{V}|} \quad (12)$$

from which we find the azimuth (ϕ) and elevation (θ) angles of the vector \mathbf{V} and will apply them to our empirical cases presented in Section 3. The generalized degree of polarization in 3D framework, P_3 , is dependent on two purity indices, P_1 and P_2 , and can be calculated from 3D Stokes parameters [13].

$$P_3 = \frac{\sqrt{\sum_{i=1}^8 \langle \Lambda_i \rangle^2}}{\sqrt{3} \langle \Lambda_0 \rangle} = \sqrt{\frac{1}{4} (3P_1^2 + P_2^2)} \quad (13)$$

The value of P_3 for a fully polarized wave is 1 and for a 2D unpolarized wave, which has a well-defined propagation direction, is equal to 0.5. P_3 is 0 for a wave with completely random direction of propagation.

3. EXPERIMENTAL RESULTS

Leveraging the formulation presented in Section 2, we now characterize the three distinct environments using polarization indices and arrival directions obtained from the 3D Stokes framework. To the best of the authors' knowledge, applying this 3D framework to data collected over frequency and space and to compare/contrast wireless environments has not been presented to date.

3.1. Methodology

The three surrogate environments represented an ideal (no multipath) environment, an office setting, and a highly reflective factory setting. To emulate an ideal setting, the testing was conducted in a compact anechoic chamber. The second environment was a non-line-of-sight condition within a lab. A compact (0.9 m \times 0.9 m \times 0.3 m) reverberation chamber was utilized to create the highly reflective scenario.

A vector network analyzer (VNA) was used to measure path loss between the two antennas. Specifically, S_{21} was measured, that is the signal power at Port 2 of the VNA (receive antenna) relative to the power at Port 1 (transmit antenna). S_{21} measurements were made at 551 frequencies between 2.40 GHz and 2.48 GHz. To emulate the random placement of the transmitting device, the transmit antenna was mounted on a linear track that allowed positioning to one of 50 repeatable locations in 1 cm (i.e., $< \lambda/10$) increments.

3.2. Summary of Results

To obtain the results presented herein, we created spectral polarization matrices for each of the 50 locations by averaging over the 551 S_{21} measurements. Using this approach we find clear distinctions between the resulting parameters for the three different environments.

Figure 1 shows the two purity indices, P_1 and P_2 , calculated along 50 positions in the three environments. We clearly see the non-ideal environments depolarize the signal. Significantly, P_2 is much less than unity indicating that the depolarization is indeed three dimensional. The mean value of purity indices over 50 positions and generalized degree of polarization are presented in Table 1. In the anechoic chamber where there is no multipath components, the shape and plane of polarization ellipse remains constant over frequency variations and resulting in values very close to 1 for P_1 , P_2 , and P_3 parameters. In the reverberation, by contrast, P_1 very low indication the polarization ellipse changes significantly over frequency. Furthermore, P_2 is very low, an indication that plane of polarization rotates randomly along frequency. In addition, P_3 is less than 0.5 (the one obtained for fully 2D unpolarized wave) that again confirms 3D nature of electromagnetic wave propagation in the chamber. The indices for the office indicate this is the intermediate case. In this scenario, on average, 26% ($1 - P_2$) of the

Table 1. Degree of polarization.

| Framework | $mean(P_1)$ | $mean(P_2)$ | $mean(P_3)$ |
|-----------|-------------|-------------|-------------|
| Anechoic | 0.97 | 0.99 | 0.97 |
| Office | 0.36 | 0.74 | 0.49 |
| RC | 0.24 | 0.48 | 0.40 |

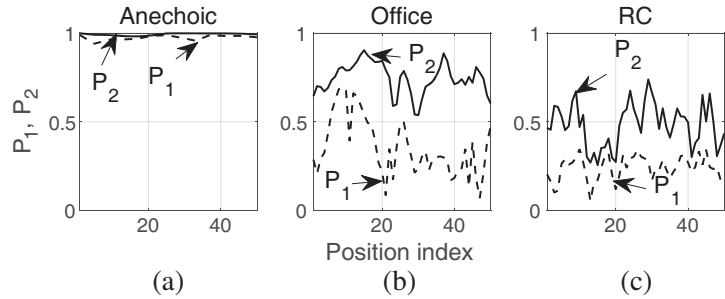


Figure 1. Polarization indices for the three demonstration environments. (a) Ideal surrogate. (b) Office surrogate. (c) Factory surrogate, reverberation chamber (RC).

total intensity of the wave behaves completely randomly along frequency and is spread uniformly in 3D sphere. This percentage is attributed to the part of the 3D polarization matrix with equal eigenvalues.

The direction of propagation was calculated from Stokes parameters, using equation Eq. (12), for the measured frequencies in the band from 2.40 to 2.48 GHz. The results are presented Fig. 2. Since there is little depolarization in the anechoic chamber, the received direction is in original transmitted plane and the depolarization angle is approximately zero. In addition, as direction of propagation is almost fixed over the frequency, this confirms the result presented for $P_2 \approx 1$ in Table 1. However, in the office setup, the rotation of polarization plane along frequency band is evident. This rotation becomes even more prominent in reverberation chamber which indicates that this environment is more frequency-dependent than the office, as the data in Table 1 confirm. The rotations in the latter two cases is an indicator that the receiver’s polarization should include all three planes in order to compensate for such depolarization effects. Recently, tripolar antennas have been developed in order to mitigate such severe multipath and depolarized channels [14, 15].

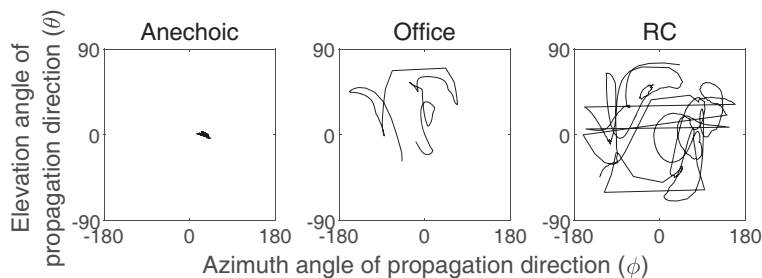


Figure 2. Azimuth and elevation angles of direction of propagation over frequency band of 2.40–2.48 GHz at one position.

4. CONCLUSION

In this work, we presented a Stokes vector-based analytical framework to study depolarization in three dimensions. We applied this framework to empirical data in order to compare and contrast depolarization seen in three distinct environments. For environments with significant multipath, our

calculated parameters show that depolarization is indeed a three dimensional effect. As wireless IoT systems become more pervasive and are deployed in evermore cluttered environments, these results can help determine if antenna systems that are tripolar are warranted. If so, then employing 3D polarization diversity in these scenarios would considerably improve link reliability as compared to the traditional dual polarization, 2D diversity approaches.

ACKNOWLEDGMENT

This material is based upon work supported by the National Science Foundation under Grant No. ECCS-1508907.

REFERENCES

1. Frolik, J., V. Sipal, and D. J. Edwards, "Leveraging depolarization to increase the link reliability for wireless sensors operating in Hyper-Rayleigh environments," *Sensors Journal*, Vol. 14, No. 8, 2442–2446, IEEE, 2014.
2. Andrews, M. R., P. P. Mitra, et al., "Tripling the capacity of wireless communications using electromagnetic polarization," *Nature*, Vol. 409, No. 6818, 316–318, 2001.
3. Ellis, J. and A. Dogariu, "On the degree of polarization of random electromagnetic fields," *Optics Communications*, Vol. 253, No. 4–6, 257–265, 2005.
4. Dennis, M. R., "A three-dimensional degree of polarization based on Rayleigh scattering," *JOSA A*, Vol. 24, No. 7, 2065–2069, 2007.
5. Dao, M.-T., V.-A. Nguyen, Y.-T. Im, S.-O. Park, and G. Yoon, "3D polarized channel modeling and performance comparison of MIMO antenna configurations with different polarizations," *IEEE Transactions on Antennas and Propagation*, Vol. 59, No. 7, 2672–2682, 2011.
6. Pratt, T. G., H. Tapse, B. Walkenhorst, and G. Acosta-Marum, "A modified XPC characterization for polarimetric channels," *IEEE Transactions on Vehicular Technology*, Vol. 60, No. 7, 2904–2913, 2011.
7. Migliaccio, M., J. J. Gil, A. Sorrentino, F. Nunziata, and G. Ferrara, "The polarization purity of the electromagnetic field in a reverberating chamber," *IEEE Transactions on Electromagnetic Compatibility*, Vol. 58, No. 3, 694–700, 2016.
8. Carozzi, T., R. Karlsson, and J. Bergman, "Parameters characterizing electromagnetic wave polarization," *Physical Review E*, Vol. 61, No. 2, 0224, 2000.
9. Bosyk, G., G. Bellomo, and A. Luis, "Polarization monotones of two-dimensional and threedimensional random electromagnetic fields," *Physical Review A*, Vol. 97, No. 2, 023804, 2018.
10. Brosseau, C. and R. Barakat, "Dimensionality of the coherency matrix in polarization optics," *Optics Communications*, Vol. 91, No. 5–6, 408–415, 1992.
11. Setälä, T., A. Shevchenko, M. Kaivola, and A. T. Friberg, "Degree of polarization for optical near fields," *Physical Review E*, Vol. 66, No. 1, 016615, 2002.
12. Sabry, R., "A novel field scattering formulation for polarimetric synthetic aperture radar: 3D scattering and stokes vectors," *Progress In Electromagnetics Research M*, Vol. 27, 129–150, 2012.
13. Gil, J. J. and I. San José, "3D polarimetric purity," *Optics Communications*, Vol. 283, No. 22, 4430–4434, 2010.
14. Ramirez, R. A., M. Golmohamadi, J. Frolik, and T. M. Weller, "3D printed on-package tripolar antennas for mitigating harsh channel conditions," *2017 IEEE Radio and Wireless Symposium (RWS)*, 62–64, IEEE, 2017.
15. Konanur, A., K. Gosalia, S. Krishnamurthy, B. Hughes, and G. Lazzi, "Increasing wireless channel capacity through MIMO systems employing co-located antennas," *IEEE Transactions on Microwave Theory and Techniques*, Vol. 53, No. 6, 1837–1844, June 2005.